Building evidence for conservation globally

# Journal of Threatened Taxa

10.11609/jott.2026.18.5.28739-29002
www.threatenedtaxa.org

26 May 2026 (Online & Print)
18(5): 28739–29002
ISSN 0974-7907 (Online)
ISSN 0974-7893 (Print)

Open Access

zooreach
Zoo Outreach Organisation
40 Years

ISSN 0974-7907 (Online); ISSN 0974-7893 (Print)

Publisher
**Wildlife Information Liaison Development Society**
www.wild.zooreach.org

Host
**Zoo Outreach Organization**
www.zooreach.org

Srivari Illam, No. 61, Karthik Nagar, 10th Street, Saravanampatti, Coimbatore, Tamil Nadu 641035, India
Registered Office: 3A2 Varadarajulu Nagar, FCI Road, Ganapathy, Coimbatore, Tamil Nadu 641006, India
Ph: +91 9385339863 | www.threatenedtaxa.org
Email: sanjay@threatenedtaxa.org



For Focus, Scope, Aims, and Policies, visit https://threatenedtaxa.org/index.php/JoTT/aims_scope
For Article Submission Guidelines, visit https://threatenedtaxa.org/index.php/JoTT/about/submissions
For Policies against Scientific Misconduct, visit https://threatenedtaxa.org/index.php/JoTT/policies_various

continued on the back inside cover

**Cover: Oil painting of Humpback Whale *Megaptera novaeangliae*. © R. Mahesh.**

Journal of Threatened Taxa | www.threatenedtaxa.org | 26 May 2026 | 18(5): 28845–28861
ISSN 0974-7907 (Online) | ISSN 0974-7893 (Print)
https://doi.org/10.11609/jott.10096.18.5.28845-28861
#10096 | Received 15 August 2025 | Final received 17 April 2026 | Finally accepted 28 April 2026



ARTICLE

# Succession of biofouling organisms on structural materials and their environmental drivers off the Kalpakkam coast, India

**Bandita Badakumar** [1], **D. Inbakandan** [2] & **P. Sriyutha Murthy** [3]

[1,2] National Facility Coastal and Marine Research, Centre for Ocean Research, Sathyabama Institute of Science and Technology, Chennai, Tamil Nadu 600119, India.
[1,3] Water & Steam Chemistry Division, Bhabha Atomic Research Centre, Kalpakkam, Tamil Nadu 603102, India.
[3] Homi Bhabha National Institute, Anushakti Nagar, Mumbai, Maharashtra 400094, India.
[1] bandita.badakumar@gmail.com, [2] inbakandan@gmail.com (corresponding author), [3] psmurthy@igcar.gov.in (corresponding author)

**Abstract:** The settlement and succession of marine fouling organisms were monitored on three structural materials—stainless steel (SS), titanium (Ti), and fibre-reinforced plastic (FRP)—over a 300-day static immersion in coastal waters of Kalpakkam along the eastern coast of India. Barnacles were found to be initial settlers, with 15 fouling species identified during the study period. The final climax community was dominated by green mussels, hydroids, and barnacles on all three substrates. Biofouling load was the highest on FRP (23.6 kg/m²), followed by SS (20.11 kg/m²) and Ti (16.19 kg/m²) after 300 days of exposure. Interestingly, green mussels colonized after 150 days of exposure signifying their preference for cues from the substratum. Correlation analysis revealed strong relationships between environmental parameters and fouling loads. Temperature and salinity were positively correlated (r = 0.874), while temperature and dissolved oxygen showed a negative correlation (r = -0.646). FRP surfaces supported the highest diversity and biomass accumulation compared to Ti and SS surfaces. Results of the study indicate material-specific differences in biofouling loads and findings have implication in the choice of material selection for cooling water system as well as for offshore aquaculture structures.

**Keywords:** Biofouling succession, coastal electric power station, coupons, cooling water systems, corrosion, environmental parameters, fouling area coverage, fibre reinforced plastic, macrofouling, microfouling, settlement, stainless steel, titanium.

**Editor:** Anonymity requested. **Date of publication:** 26 May 2026 (online & print)

**Citation:** Badakumar, B., D. Inbakandan & P.S. Murthy (2026). Succession of biofouling organisms on structural materials and their environmental drivers off the Kalpakkam coast, India. *Journal of Threatened Taxa* 18(5): 28845–28861. https://doi.org/10.11609/jott.10096.18.5.28845-28861



**Funding:** The financial grant for this work was provided from the Board of Research in Nuclear Sciences, Department of Atomic Energy, Government of India, funded research project entitled "Development of antifouling technologies against green mussel fouling for process cooling water system of MAPS", to Dr. D. Inbakandan, Sanction NO 56/14/03/2020-BRNS/36152.

**Competing interests:** The authors declare no competing interests.

**Declaration of competing interest:** The authors declare that they have no known competing financial interests or personal relationships that could have appeared to influence the work reported in this paper.

**Author details:** Bandita Badakumar: senior research fellow in Sathyabama Institute of Science and Technology, working for BRNS funded project titled "Development of antifouling technologies against green mussel fouling for process cooling water system of MAPS". Currently working in the field of marine ecology, biofoluing, ecotoxicology and biomarkers. D. Inbakandan: head and professor of National Facility for Coastal and Marine Research, Center for Ocean Research, at Sathyabama Institute of Science and Technology. Expert in marine biology, ecology, aquaculture and fisheries. P. Sriyutha Murthy: scientific officer and professor HBNI- BARC Facilities, Kalpakkam. Extensively worked in Biofouling control in Industrial cooling water system. Expert in biofouling, biofilms, antifouling technologies, and ecotoxicology.

**Author contribution:** BB—conceptualization, field work, sampling and formal analysis, data analysis, statistics, writing original manuscript. DI—funding, manuscript review. PSM—conceptualization, field work, manuscript review.

**Acknowledgments:** The authors would also like to thank the head, Water & Steam Chemistry Division for providing necessary facilities to carry out the research work. The authors would also like thank the Station Director of MAPS, Kalpakkam for providing the permission and support to carryout this work.

## INTRODUCTION

Marine biofouling is a ubiquitous and spontaneous process, beginning with the formation of a primary organic film, followed by microbial and algal adhesion, biofilm formation with extracellular polymeric substances (EPS) (More et al. 2014; Decho & Gutierrez 2017; Negm et al. 2019), and eventual settlement and succession of marine invertebrate larvae (Maki & Mitchell 2002; Wigglesworth-Cooksey & Cooksey 2005; Qian et al. 2007; Hadfield 2011). Succession in fouling communities is influenced by seasonality (Briand et al. 2017; Qian et al. 2022), temperature, salinity, and hydrodynamic conditions (Alotaibi & Bukhari 2021; Jamieson & Leterme 2021; Briand et al. 2022). Biofouling causes significant operational problems in industrial cooling water systems and hence control measures can be devised only after understanding the density, diversity, and seasonal settlement of fouling organisms at a given geographical location. Operational and economic losses due to biofouling are well documented in desalination plants (Azis et al. 2001; Henderson 2010; Alayande et al. 2022), power plant cooling water systems (Nair et al. 1999; Satpathy et al. 2010; Murthy et al. 2011; Rao et al. 2015), aquaculture installations (Durr & Watson 2010; Fitridge et al. 2012; Hopkins et al. 2021), offshore oil and gas platforms (Sanders et al. 2005; Yeo et al. 2009; Page et al. 2010), sensors and data buoys (Zhang et al. 2015; Venkatesan et al. 2017), and shipping (Schultz et al. 2011). Biofouling on ship hulls has been linked to the spread of invasive or non-indigenous species, causing ecological imbalance (Fernandes et al. 2016; Shevalkar et al. 2020; Yousef & Nasser 2023).

Titanium (Ti), stainless steel-304 (SS), and fibre-reinforced plastic (FRP) are widely used industrial materials, particularly in marine and coastal industries, due to their superior mechanical properties. Titanium is used as a heat transfer material, in heat exchangers at power plants in Kalpakkam, due to its excellent heat transfer and anticorrosion properties. However, it is prone to severe biofouling. SS-304 is used as a structural material in various pipelines and seawater pump casings along with FRP. Cost involved in maintaining the cooling system, heat exchangers, and structural materials is considerable (Todd et al. 2019; Wahl 2020) and therefore understanding the endemic species, their settlement, recruitment, and succession patterns on these structural materials is required to devise a suitable control strategy.

The southeastern coast of India supports a rich and diverse marine ecosystem (Satpathy et al 1996; Sahu et al. 2015; Ponnusamy et al. 2017). Several studies have characterized various aspects of this environment, including microbial diversity and the settlement and succession of biofouling organisms off the Kalpakkam coast (Nair et al. 1988; Rajagopal et al. 1997; Sahu et al. 2011, 2015). These investigations have consistently identified major macrofouling species such as barnacles, mussels, and ascidians in the region. While building upon these earlier findings, the present study provides an updated perspective by recording monthly biofouling load on different structural materials and documenting the seasonal succession of fouling communities. In contrast to earlier works, this study integrates environmental drivers (such as, temperature, salinity, dissolved oxygen, nutrients, and chlorophyll concentration) to examine their correlation with observed fouling trends. Notably, fluctuations in fouling community composition during the post-monsoon period appear to be influenced by changes in temperature and reduced nutrient availability (Venugopalan 1991; Venkatnarayanan 2018). This combined approach not only reaffirms previously observed patterns but also offers new insights into the environmental drivers that shape biofouling dynamics in this ecologically and industrially important coastal zone.

The present study evaluates biofouling accumulation and community succession on three structural materials (Ti, SS, and FRP) deployed in the coastal waters off Kalpakkam on the southeastern coast of India. The objective includes assessing the temporal variation in biofouling load and species composition over a one-year period; monitoring monthly settlement and succession patterns of fouling organisms; and correlating these patterns with variations in physicochemical parameters. The study further seeks to understand the timing and dynamics of organism settlement and its relationship with environmental conditions, providing insights into material-specific fouling behaviour in a tropical marine environment.

## MATERIALS AND METHODS

### Description of study area and coupon immersion

The study was carried out from January to December 2022 at the approach jetty area of MAPS an operating coastal power station, off Kalpakkam (12.335$^{o}$ N, 80.115$^{o}$ E) located on the eastern coast, of India (Image 1). Coupon mounted on holder with stainless steel screws were suspended at a distance of 350 m from the shore beyond the coastal surf zone at a depth of -1 m . Three different structural materials most commonly used in industry were used as coupons for the experiment such as stainless steel

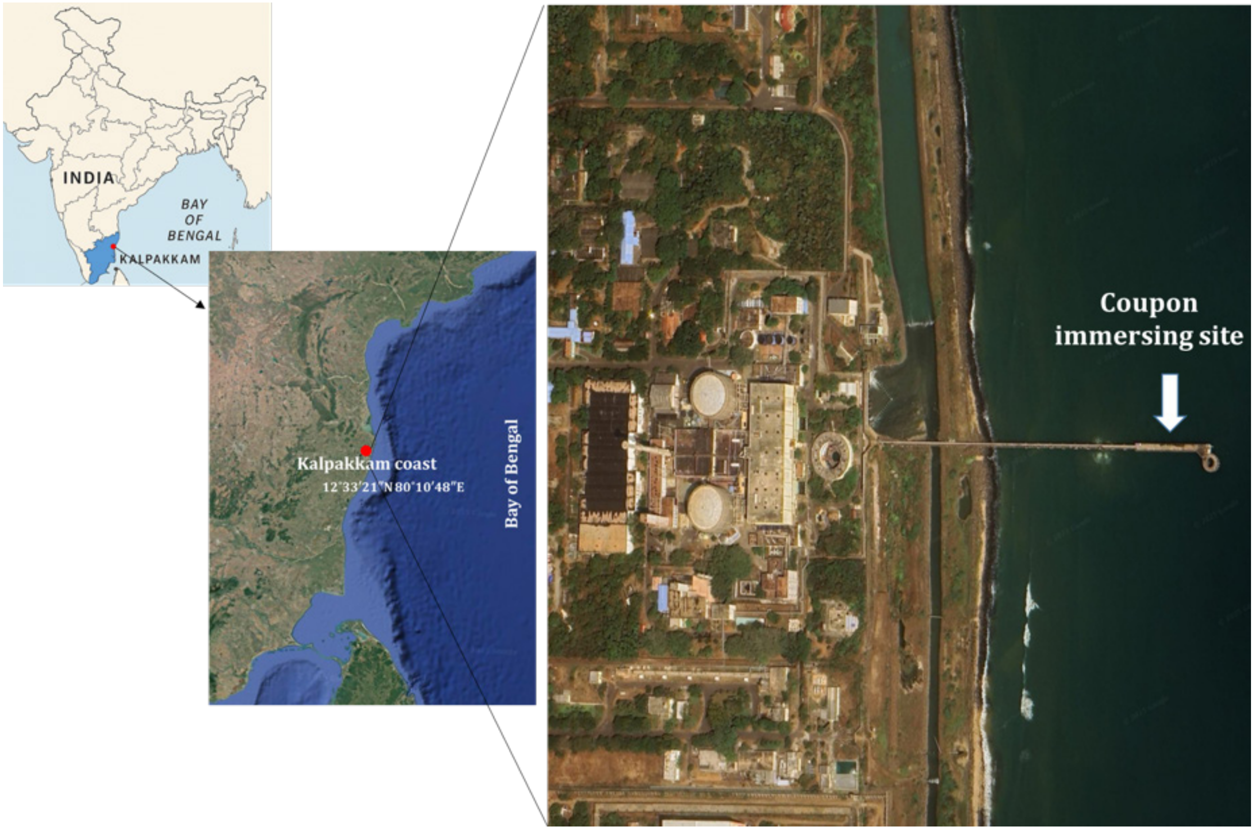


Image 1. Map showing the coupon immersing site in the Madras Atomic Power Station (MAPS) (Source: Google Earth).

304 (SS-304), titanium (Ti), and fibre-reinforced plastic (FRP) with a size of 10 × 15 cm. Each coupon (in triplicate) was attached on a polypropylene frame and suspended at a depth of -1.0 m in coastal waters. The settlement pattern and succession of macrofouling organisms was monitored monthly on the coupons, for a period of 300 days. Every month the coupons were retrieved for checking the wet biomass and photographed (Canon, DS EOS RP) for the species composition. The percentage coverage of different organisms was estimated using Image J software (NIH, USA). The same set of coupons was monitored throughout the study period, with monthly retrieval for non-destructive assessment of biofouling (photography and wet weight estimation). Care was taken during handling and measurement to minimize disturbance, and the coupons were promptly re-immersed to allow continued development of the fouling community. Barnacles, polychaete tube worms, bivalves, and other organisms (such as crabs, snails) were counted individually and expressed as individuals/$cm^2$. Coelenterate hydroids, ascidians, and encrusted bryozoans, being colonial organisms, were counted as area occupied per $cm^2$ on each of the coupons.

**Measurement of environmental parameters**

Physico-chemical parameters such as salinity, water temperature, pH, and dissolved oxygen (DO), were measured by using a multi-parameter water quality probe in seawater (HYDROLAB, DS5, USA). Chlorophyll a (Chl-a) concentration was determined by filtering 500 mL seawater through a Whatman GF/C glass fibre filter. The filter papers were then placed in 90% acetone (10 ml) and incubated at 4˚ºC in complete darkness for overnight to facilitate pigment extraction. The absorbance of the extracted solution was subsequently measured using a spectrophotometer to quantify the chlorophyll-a concentration. During the study period, sub-surface seawater samples were collected monthly from the coastal waters, transported to laboratory for the estimation of nutrient parameters viz: nitrite ($NO_2$), nitrate ($NO_3$), inorganic phosphate ($PO_4$), ammonia ($NH_3$), and silicate (Si) by following the standard method as described by Grasshoff et al. (1999). Total suspended solids (TSS) was estimated in water sample as per the gravimetric method (APHA 2005).

**Statistical analysis**

All samples were collected in triplicate and the measured values were expressed as mean with standard deviation. To evaluate the significant differences with physico-chemical parameters between different seasons were analyzed using one-way ANOVA using PAST- 4.03 software (UK) (Hammer et al. 2001). SPSS (version 10) software stats package was used for generating the minimum, maximum, mean and SD values with ANOVA *p*-values. Pearson correlation matrix was generated using PAST-4.03 software for *p*-values. Fouling load on the surface of coupons were quantified using ImageJ software (NIH, USA).

## RESULTS AND DISCUSSION

### Hydrobiology and species diversity

During the study, 15 species were identified across all three coupons, representing seven distinct phyla: Annelida (2 species), Arthropoda (3 species), Cnidaria (1 species), Ectoprocta (1 species), Mollusca (5 species), Echinodermata (1 species), and Urochordata (3 species) (Table 1) (Rajagopal et al. 1997; Venkatnarayanan 2018). Monthly observations revealed a notable dominance of hydroids, green mussels, and barnacles, reflecting their competitive advantage and prevalence within the fouling communities in this geographical location (Sahu et al. 2011; Venkataraman et al. 2012). Various epibiotic organisms such as crab, polychaete worms, amphipods and gastropods were also observed (Wickramasinghe et al. 2021). The species richness recorded on the panels (mean ± standard deviation) fluctuated based on the type of substrate and season.

Table 2 presents seasonal variations in physico-chemical and biological parameters, which were prominent throughout the study period, with fluctuations across different seasons observed at Kalpakkam on the southeastern coast of India. The categories are monsoon (MON: June–September), post-monsoon (POM: October–December), and pre-monsoon (PRM: January–May).. Seawater temperatures were lowest in the month of December (26.3 °C, POM) and January (26.5 °C, PRM), while the highest was observed in April and May (30.2—31.0 °C) in PRM season. A steady decline in water temperature occurred during the MON season (June to August), followed by a marginal rise during the POM phase (September–October), which then continued to increase during the subsequent pre-monsoon months. Earlier studies at the intake region of the power plant site reported fluctuation of temperature ranging from minimum 5.8 °C to maximum 8.0 °C (Sahu et al. 2012; Venkatnarayanan 2018). Previous studies on sea-surface temperature variability have well established the role of atmospheric temperature impacts on sea-surface temperature, which significantly influence the later leading to seasonal and regional variations (Deser et al. 2010). Temperature fluctuation can have cascading effects on chemical and biological process, affecting salinity, phytoplankton growth, and conductivity (Satheesh & Wesley 2009; Fernandez et al. 2022). Current findings align with the earlier observations regarding air temperature along the study area, which exhibited a bimodal pattern with peaks occurring in April–May and another during September–October.

The pH levels in Kalpakkam coastal waters ranged 8.07–8.26 across the three seasons, suggesting a generally well-buffered aquatic ecosystem, while salinity exhibited seasonal variation, reaching its lowest at 27.6 ppt in December and peaking to 35.4 ppt in June (summer). The lowest pH and salinity recorded in December (POM) are attributed to a large inflow of rainwater during the north-east monsoon (NEM) from both Sadras and Edayur estuarine systems (Venkatnarayanan 2018). The highest pH value (8.24) was recorded in July during the monsoon period. These fluctuations in pH and salinity may be linked to the north-east monsoon, with additional influences from freshwater influx from nearby estuarine systems and also due the influx of low-saline Palar riverine water (Varkey et al. 1996; Sahu et al. 2011). Dissolved oxygen (DO) was highest in post-monsoon (November, 6.91 mg/L) and lowest in the month of September (5.23 mg/L), reflecting seasonal changes. The peak DO levels were observed during month of November may be attributed to an increase in chlorophyll-*a* concentration, driven by the northeast monsoon and the influx of nutrient-rich estuarine waters (Satpathy 1996). Additionally, the reduction in salinity and enhanced oxygenation in large tidal action resulting from physical mixing processes could have further contributed to the elevated DO levels (Venkatnarayanan 2018).

Chlorophyll-*a* fluctuated between 6.3 mg $L^{-1}$ (Oct) and 18.6 (Jun) mg $L^{-1}$, an indicator of phytoplankton growth, reflecting favourable conditions for algal growth due to nutrient availability (Rajagopal et al. 1991). Highest concentration was observed during pre-monsoon period and at the beginning of the monsoon period, which may be attributed to the relatively stable and optimal conditions of salinity, temperature, light, and nutrient levels prevailing during this period (Sahu et al. 2011). The low chlorophyll-a levels observed during the monsoon season may be attributed to reduced salinity, which is most likely unfavourable for marine phytoplankton growth, while the minimum concentration recorded in

**Table 1. Composition of biofouling community on coupons.**

| Phylum | Class | Order | Family | Species |
|---|---|---|---|---|
| Annelida | Polychaeta | Canalipalpata | Serpulidae | *Hydroides elegans* |
| | | Aciculata | Nereididae | *Pseudonereis* sp. |
| Arthropoda | Cirripedia | Thoracica | Balanidae | *Amphibalanus reticulatus* *Balanus amphitrite* |
| | Malacostaca | Amphipoda | Corophidae | *Corophium* sp. |
| Cnidaria | Hydrozoa | Thecata | Campanulariidae | *Obelia dichotoma* |
| Ectoprocta | Gymnolaemata | Cheilostomata | Bugulidae | *Bugula* sp. |
| Mollusca | Bivalvia | Mytilida | Mytilidae | *Perna viridis* |
| | | | Ostreidae | *Modiolus modiolus* |
| | | | | *Crassostrea madrasensis* |
| | Gastropoda | Neogastropoda | Muricidae | *Thais* sp. |
| | | | Patellidae | *Patella* sp. |
| Echinodermata | Ophiurodea | Ophiurida | Ophiotrichidae | *Ophiothrix* sp. |
| Urochordata | Ascidiacea | Enterogona | Didemnidae | *Didemnum* sp. |
| | | Aplousobranchia | | *Lissoclinum* sp. |
| | | Phlebobranchia | Perophoridae | *Ecteinascidia* sp. |

October (6.23 mg $L^{-1}$) could be due to increased grazing pressure. Several studies conducted along the Kalpakkam coast have reported similar trends to those observed in the present study (Rajagopal et al. 1991; Satpathy 1996; Sahu et al. 2015; Achary et al. 2010; Venkatnarayanan 2018). Levels of total suspended solids (TSS) was found to be high during the month of November (88 mg $L^{-1}$), indicating a significant ($p < 0.001$) increase in sediment resuspension during post-monsoon period, while the lowest values were recorded in the month of August (29.3 mg$L^{-1}$). Nutrient concentrations, including nitrite, nitrate, ammonia, phosphate, and silicate, showed significant seasonal variation, with higher levels during the monsoon and post-monsoon periods, followed by a noticeable decline toward the end of the pre-monsoon season. The concentration for nitrate and nitrite was 5.18—9.45 µmol $L^{-1}$ and 1.0—3.08 µmol $L^{-1}$, respectively. Levels of ammonia varied 1.0—3.7 µmol $L^{-1}$, maintaining a relatively consistent concentration across all seasons. Levels of inorganic phosphate ranged 1.68—5.7 µmol $L^{-1}$ during all seasons. A significant ($p < 0.001$) rise in phosphate concentration was observed during MON and POM period, with a steady increase from August to December. However, the phosphate concentration spiked during the month of December (14.1 µmol $L^{-1}$), which could be due to the NEM rains which induced land runoff. This trend may be attributed to the phenomenon of 'coastal upwelling' which has been frequently reported in this region (Suryanarayan & Rao 1992). The silicate (Si) concentration was found relatively high in the POM with a value of 19.18 µmol $L^{-1}$ compared to the other two seasons MON and PRM. The silicate level ranged 11.04—19.18 µmol $L^{-1}$ throughout three seasons. This parameter also in turn coincides with the mixing of the backwater due to the NEM rains (Sahu et al. 2012).

ANOVA results indicate statistically significant seasonal variations ($p \leq 0.05$) in most parameters, including temperature, salinity, dissolved oxygen, chlorophyll-a, TSS, and nutrient concentrations, while silicate ($p = 0.742$) remained relatively stable. These findings highlight the influence of seasonal changes on water quality, with monsoon-driven fluctuations affecting salinity, nutrients, and biological activity. These findings underscore the dynamic influence of seasonal cycles on water quality, with monsoonal rainfall playing a crucial role in nutrient loading, salinity dilution, and biological productivity. The data suggest that freshwater inflows, evaporation, and biological interactions collectively shape the physicochemical characteristics of the aquatic system, highlighting the need for continuous monitoring to assess ecosystem health and potential anthropogenic impacts.

## Biofouling loading on structural materials

The physical and chemical characteristics of structural materials play a crucial role in determining their susceptibility to biofouling. In the present study, distinct differences were observed in fouling intensity

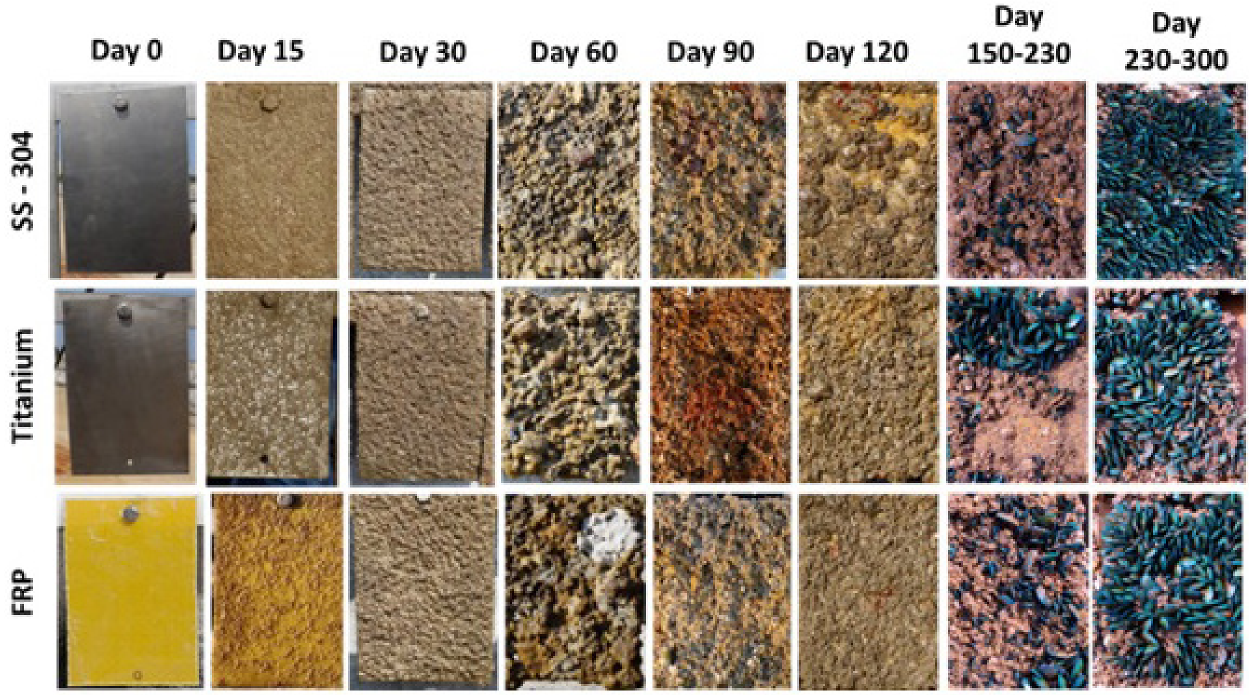


Image 2. Biofouling organisms observed on different structural materials (SS—stainless steel | Ti—titanium | FRP—fibre reinforced plastic) immersed in Kalpakkam coastal waters from Day 0 to 300.

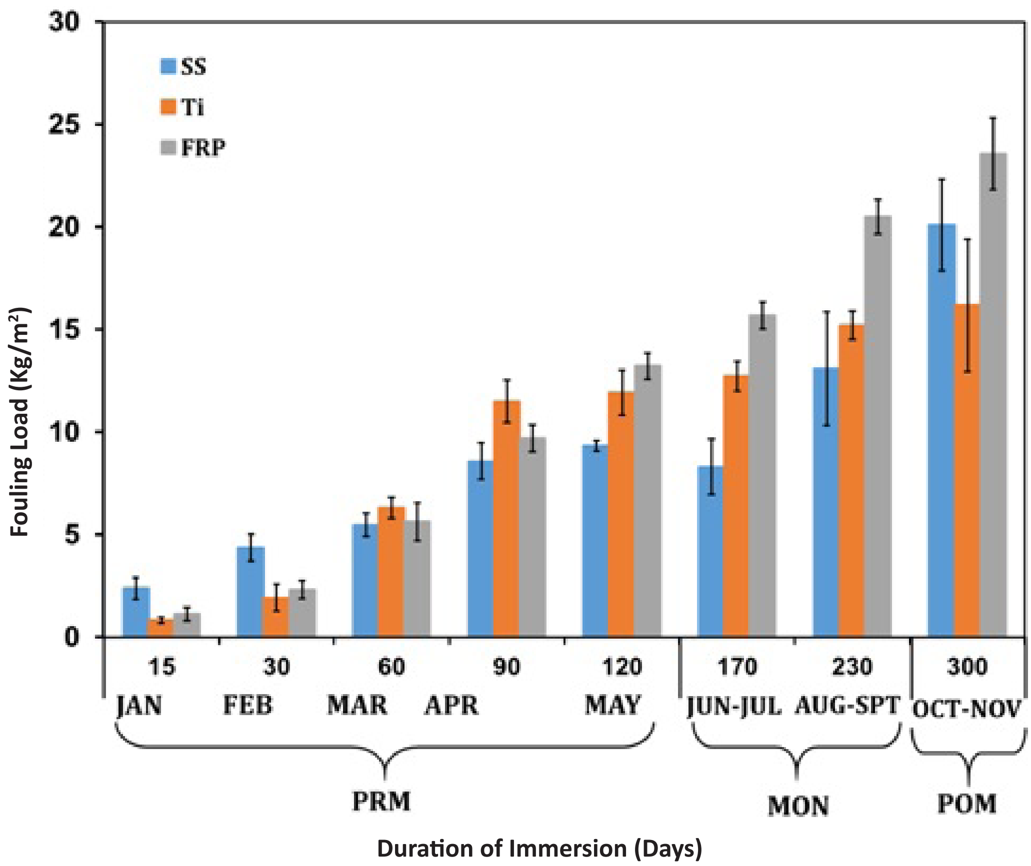


Figure 1. Temporal variation of biofouling loading observed on different structural material (SS—stainless steel | Ti—titanium | FRP—fibre reinforced plastic) with respect to seasonal variation (PRM—pre-monsoon | MON—monsoon | POM—post-monsoon) of fouling load.

among stainless steel (SS), titanium (Ti), and fibre-reinforced plastic (FRP), which can be attributed to their surface properties. Stainless steel possesses a relatively smooth surface with moderate surface energy, allowing initial microbial and larval attachment. However, the passive oxide layer formed on its surface provides a certain degree of corrosion resistance and reduces long-term colonization (Rajagopal et al. 1997; Dexter & Chandrasekaran 1998). Titanium, exhibits superior anticorrosive properties due to the formation of a stable and highly inert titanium oxide ($TiO_2$) film, which minimizes both corrosion and bio-adhesion (Kobayashi & Dauskardt 2001; Dobretsov 2010). Its low surface roughness and hydrophobic nature further contribute to its resistance to organism settlement (Zhao et al. 2014). Fibre-reinforced plastic on the other hand, has a comparatively rough and heterogeneous surface structure that provides micro-crevices for the attachment of fouling organisms (Patil et al. 2007; Ponnusamy et al. 2016). Its inert nature and surface irregularities create favourable conditions for larval settlement and growth of macrofouling communities. Consequently, FRP showed the highest fouling load in the present study, while titanium exhibited the least. These findings underscore that the surface texture, energy, and chemical composition of materials strongly influence initial colonization, community succession, and the overall biofouling load in marine environments (Callow & Callow 2011; Dobretsov et al. 2013).

Biofouling loading on different structural materials SS, Ti, and FRP, immersed over a period of 300 days in Kalpakkam coastal waters is given in Image 2. Larval settlement on all three substrates was found to occur within the first 24 hours of immersion. However, with time, shifts in community structure and species succession lead to dynamic changes in the fouling assemblage. A total of 15 organisms were identified on different substrates during the study period, with barnacles emerging as the initial settlers, rapidly colonizing the surfaces within the first 1–4 days of immersion. In addition to barnacles, other fouling species, including ascidians, bryozoans, oysters, and gastropods were also present. Various epizoic organisms such as crabs, copepods, brittle stars, and amphipods were also present. Barnacles and hydroids were found to attach between the 5$^{th}$ and 7$^{th}$ day of immersion whereas, settlement of oysters and polychaetes occurred later, establishing themselves between the 7$^{th}$ and 10th day of immersion. Even though green mussels spat settlement was detected as early as the 15$^{th}$ day of immersion, juvenile recruitment was observed only after 120–230 days of immersion. Rajagopal et al. (1997) similarly reported juvenile mussel settlement during May–June and October. In the present study, the juveniles that are settled after 120 days, eventually overgrew, covered the previously settled fouling organism on the coupons, a pattern previously reported along the same coast (Rajagopal et al. 1997; Sahu et al. 2011). Similar kind seasonal succession of green mussel pattern and fouling load were observed in the same coast (Rajagopal et al. 1997; Sahu et al. 2013; Venkatnarayanan 2018; Rao et al. 2021 ).

The settlement and recruitment of different biofouling organisms on different materials, season wise is given in Figure 1. Biofouling loading, increased with time on all three surfaces. However, there were significant differences in the intensity of colonization of different fouling species, between the three surfaces. Fibre-reinforced plastic (23.6 kg/m$^2$) surface exhibited the highest fouling accumulation, consistently compared to SS (20.11 kg/m$^2$) and Ti (16.19 kg/m$^2$) over the immersion period. Within the 120$^{th}$ day of immersion, fouling load on FRP surfaces reached (13 kg/m$^2$) which was significantly higher ($p < 0.05$). This increased to 15.67 kg/m$^2$ by the 170$^{th}$ day, with fouling accumulation accelerating even further, ultimately reaching 23.6 kg/m$^2$ by 300 days. The increased fouling on FRP suggests may be attributed to the surface texture and material properties which provide a more favourable substrate for marine organisms to attach and grow (Venkatnarayanan 2018).

Initial loading of stainless steel (9.2 kg/m$^2$), were much similar to that observed with FRP (9.72 kg/m$^2$) surfaces but diverged around 90–120 days. By 300 days, SS accumulated a fouling load of 20.11 kg/m$^2$ marginally lower compared to FRP (23.57 kg/m$^2$) but higher than Ti (16.19 kg/m$^2$), indicating, the surface was not immune to biofouling. Results suggests that SS surfaces in marine environment may still require protection by use of antifouling coatings for long-term applications. On the other hand, Ti surface was found to attract consistently low settlement and recruitment of fouling organism compared to both SS and FRP throughout the 300-day immersion period. This reduced settlement observed on titanium surfaces is likely due its smooth surface and formation of a passive oxide layer, which inhibit the attachment of marine organisms, making it the most suitable material for long-term marine applications.

**Percentage of area coverage on different coupons**

A comprehensive analysis of settlement and recruitment of biofouling organisms (Figure 2a,b,c) on SS, Ti, and FRP revealed that species settlement on SS

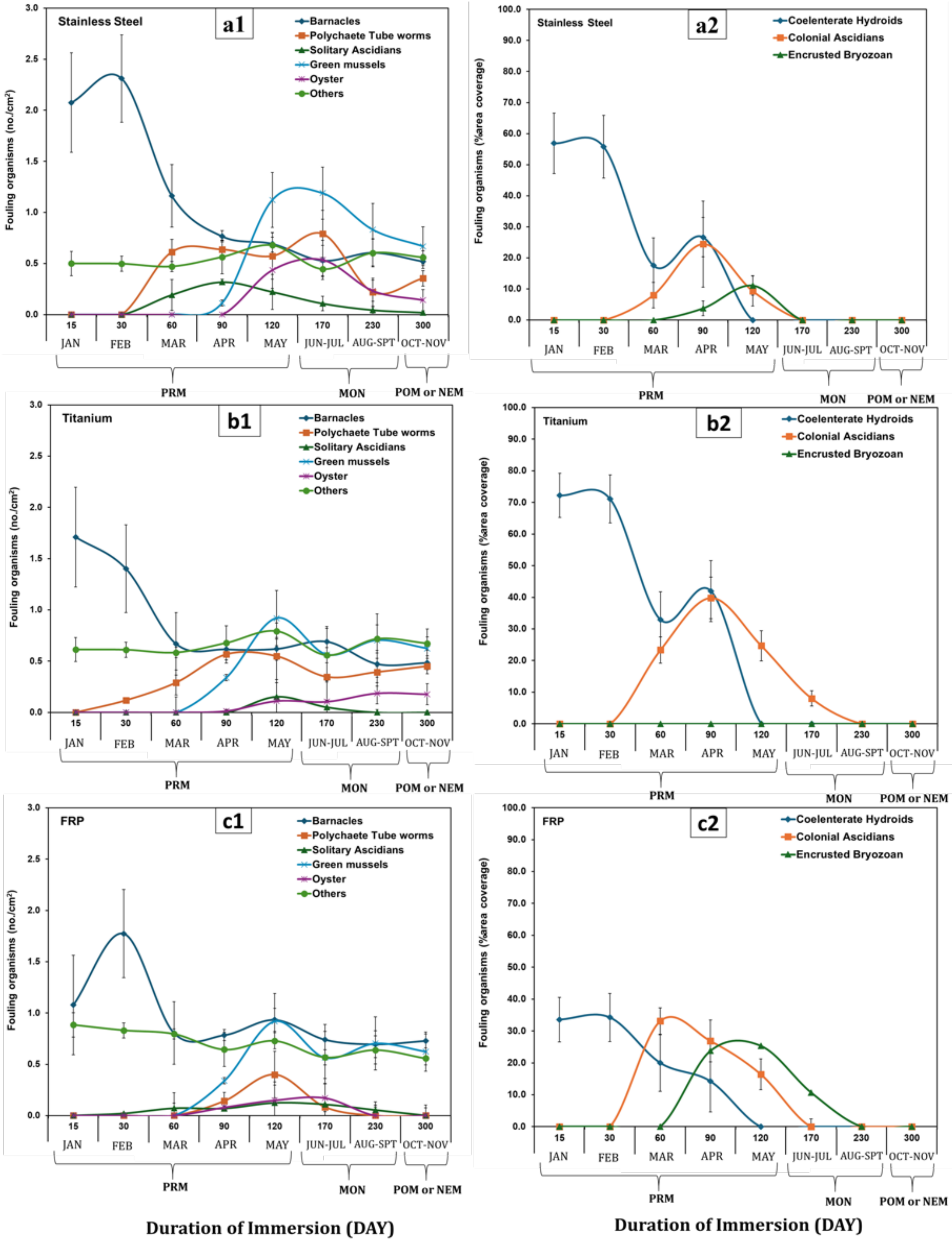


**Figure 2. Biofouling load and percent area coverage observed on different coupons: a1 & a2—stainless steel | b1 & b2—titanium | c1 & c2—fibre reinforced polymer throughout the year in three seasons.**

Table 2. Hydro-biological parameters observed in the coastal waters of Kalpakkam from January to December 2022, representing three distinct seasonal periods.

| Season | Month | | WT (°C) | pH | Salinity (PPT) | DO (mg/L) | Chl-*a* (mg $L^{-1}$) | TSS (mg $L^{-1}$) | $NO_3$ (µmol $L^{-1}$) | $NO_2$ (µmol $L^{-1}$) | $NH_3$ (µmol $L^{-1}$) | IP (µmol $L^{-1}$) | Si (µmol $L^{-1}$) |
|---|---|---|---|---|---|---|---|---|---|---|---|---|---|
| MON | August | Minimum | 27.30 | 8.09 | 34.21 | 5.84 | 9.12 | 23.00 | 7.21 | 1.25 | 1.65 | 4.23 | 11.25 |
| | | Maximum | 27.90 | 8.17 | 34.45 | 5.96 | 9.58 | 36.00 | 7.45 | 1.43 | 1.85 | 4.54 | 12.34 |
| | | Mean | 27.60 | 8.13 | 34.30 | 5.89 | 9.35 | 29.33 | 7.33 | 1.35 | 1.75 | 4.37 | 11.86 |
| | | SD | 0.30 | 0.04 | 0.13 | 0.06 | 0.23 | 6.51 | 0.12 | 0.09 | 0.10 | 0.16 | 0.55 |
| | July | Minimum | 26.20 | 8.22 | 34.58 | 5.67 | 7.39 | 26.00 | 6.34 | 1.04 | 3.45 | 3.42 | 15.45 |
| | | Maximum | 27.30 | 8.26 | 34.96 | 5.89 | 7.89 | 34.00 | 6.95 | 1.14 | 3.99 | 3.67 | 15.87 |
| | | Mean | 26.95 | 8.24 | 34.81 | 5.77 | 7.61 | 29.67 | 6.71 | 1.09 | 3.70 | 3.51 | 15.34 |
| | | SD | 0.36 | 0.03 | 0.20 | 0.11 | 0.25 | 4.04 | 0.33 | 0.05 | 0.27 | 0.14 | 1.74 |
| | June | Minimum | 26.90 | 8.08 | 35.23 | 5.42 | 18.43 | 32.00 | 5.11 | 0.86 | 2.63 | 1.56 | 17.54 |
| | | Maximum | 26.30 | 8.18 | 35.67 | 5.62 | 18.88 | 48.00 | 5.29 | 1.11 | 2.96 | 1.87 | 17.35 |
| | | Mean | 26.50 | 8.13 | 35.45 | 5.53 | 18.61 | 40.67 | 5.19 | 1.01 | 2.82 | 1.69 | 17.59 |
| | | SD | 0.40 | 0.05 | 0.22 | 0.10 | 0.24 | 8.08 | 0.09 | 0.13 | 0.17 | 0.16 | 3.46 |
| | September | Minimum | 27.90 | 8.12 | 33.43 | 5.23 | 9.89 | 47.00 | 7.69 | 1.45 | 2.54 | 4.56 | 12.35 |
| | | Maximum | 28.50 | 8.15 | 34.69 | 5.46 | 10.12 | 65.00 | 7.88 | 1.68 | 2.87 | 4.87 | 12.96 |
| | | Mean | 28.27 | 8.14 | 34.23 | 5.34 | 10.00 | 57.00 | 7.78 | 1.56 | 2.72 | 4.71 | 12.62 |
| | | SD | 0.32 | 0.02 | 0.70 | 0.12 | 0.12 | 0.92 | 0.10 | 0.12 | 0.17 | 0.16 | 0.93 |
| POM | December | Minimum | 27.80 | 8.08 | 27.45 | 6.45 | 10.98 | 53.00 | 7.58 | 1.55 | 2.45 | 5.59 | 19.87 |
| | | Maximum | 26.80 | 8.14 | 27.84 | 6.89 | 11.54 | 68.00 | 7.98 | 1.89 | 2.87 | 5.87 | 19.78 |
| | | Mean | 26.30 | 8.11 | 27.66 | 6.70 | 11.25 | 59.00 | 7.73 | 1.70 | 2.62 | 5.70 | 19.18 |
| | | SD | 0.50 | 0.02 | 0.20 | 0.22 | 0.28 | 0.94 | 0.22 | 0.17 | 0.22 | 0.15 | 0.48 |
| | November | Minimum | 27.20 | 8.18 | 28.35 | 6.54 | 8.56 | 79.00 | 9.32 | 3.45 | 0.87 | 5.24 | 13.56 |
| | | Maximum | 27.70 | 8.23 | 28.79 | 7.23 | 8.87 | 98.00 | 9.67 | 3.75 | 1.12 | 5.49 | 13.45 |
| | | Mean | 27.47 | 8.21 | 28.53 | 6.92 | 8.70 | 88.00 | 9.45 | 3.62 | 1.02 | 5.37 | 13.83 |
| | | SD | 0.55 | 0.03 | 0.23 | 0.35 | 0.16 | 0.54 | 0.19 | 0.16 | 0.13 | 0.13 | 0.10 |
| | October | Minimum | 27.30 | 8.07 | 30.12 | 6.21 | 6.23 | 68.00 | 8.45 | 2.68 | 1.24 | 4.45 | 11.28 |
| | | Maximum | 27.90 | 8.16 | 30.42 | 6.49 | 6.54 | 89.00 | 8.94 | 2.84 | 1.64 | 4.67 | 11.54 |
| | | Mean | 27.63 | 8.11 | 30.26 | 6.36 | 6.37 | 76.33 | 8.68 | 2.77 | 1.41 | 4.56 | 11.05 |
| | | SD | 0.31 | 0.05 | 0.15 | 0.14 | 0.16 | 0.15 | 0.25 | 0.08 | 0.21 | 0.11 | 0.65 |

| Season | Month | | WT (˚C) | pH | Salinity (PPT) | DO (mg/L) | Chl-*a* (mg L$^{-1}$) | TSS (mg L$^{-1}$) | $NO_3$ (µmol L$^{-1}$) | $NO_2$ (µmol L$^{-1}$) | $NH_3$ (µmol L$^{-1}$) | IP (µmol L$^{-1}$) | Si (µmol L$^{-1}$) |
|---|---|---|---|---|---|---|---|---|---|---|---|---|---|
| PRM | April | **Minimum** | 30.90 | 8.13 | 34.54 | 5.46 | 15.22 | 70.00 | 5.32 | 0.95 | 3.11 | 2.21 | 15.21 |
| | | **Maximum** | 29.50 | 8.21 | 34.98 | 5.89 | 15.68 | 78.00 | 5.63 | 1.12 | 3.57 | 2.37 | 15.24 |
| | | **Mean** | 30.20 | 8.17 | 34.69 | 5.70 | 15.45 | 74.33 | 5.47 | 1.05 | 3.32 | 2.29 | 15.63 |
| | | **SD** | 0.30 | 0.04 | 0.25 | 0.22 | 0.23 | 4.04 | 0.16 | 0.09 | 0.23 | 0.08 | 0.54 |
| | February | **Minimum** | 28.90 | 8.14 | 31.25 | 6.12 | 15.32 | 58.00 | 8.23 | 2.89 | 2.23 | 4.35 | 15.34 |
| | | **Maximum** | 28.90 | 8.21 | 31.63 | 6.59 | 15.89 | 68.00 | 8.56 | 3.24 | 2.56 | 4.51 | 15.27 |
| | | **Mean** | 28.37 | 8.18 | 31.38 | 6.31 | 15.62 | 63.00 | 8.41 | 3.08 | 2.43 | 4.44 | 15.99 |
| | | **SD** | 0.50 | 0.04 | 0.22 | 0.25 | 0.29 | 0.60 | 0.17 | 0.18 | 0.17 | 0.08 | 0.11 |
| | January | **Minimum** | 26.70 | 8.13 | 29.23 | 6.09 | 8.23 | 49.00 | 7.98 | 2.12 | 1.45 | 3.12 | 14.63 |
| | | **Maximum** | 26.80 | 8.15 | 29.40 | 6.42 | 8.96 | 59.00 | 8.16 | 2.29 | 1.86 | 3.25 | 14.23 |
| | | **Mean** | 26.53 | 8.14 | 29.32 | 6.25 | 8.55 | 54.67 | 8.06 | 2.22 | 1.69 | 3.17 | 14.04 |
| | | **SD** | 0.25 | 0.01 | 0.09 | 0.17 | 0.37 | 0.51 | 0.09 | 0.09 | 0.21 | 0.07 | 1.31 |
| | March | **Minimum** | 30.08 | 8.08 | 32.48 | 5.23 | 18.23 | 62.00 | 7.54 | 1.05 | 2.54 | 3.56 | 14.35 |
| | | **Maximum** | 30.05 | 8.18 | 32.96 | 5.65 | 18.76 | 70.00 | 7.86 | 1.26 | 2.89 | 3.95 | 14.54 |
| | | **Mean** | 30.08 | 8.13 | 32.71 | 5.48 | 18.48 | 65.33 | 7.69 | 1.15 | 2.77 | 3.76 | 14.41 |
| | | **SD** | 0.36 | 0.05 | 0.24 | 0.22 | 0.27 | 0.42 | 0.16 | 0.11 | 0.20 | 0.20 | 0.10 |
| | May | **Minimum** | 32.30 | 8.09 | 34.57 | 5.67 | 17.23 | 74.00 | 6.35 | 1.03 | 3.18 | 2.54 | 14.27 |
| | | **Maximum** | 31.80 | 8.18 | 34.72 | 5.84 | 17.52 | 81.00 | 6.59 | 1.20 | 3.46 | 2.78 | 15.62 |
| | | **Mean** | 31.05 | 8.13 | 34.63 | 5.78 | 17.40 | 78.00 | 6.46 | 1.12 | 3.31 | 2.67 | 15.18 |
| | | **SD** | 0.25 | 0.05 | 0.08 | 0.09 | 0.15 | 0.61 | 0.12 | 0.09 | 0.14 | 0.12 | 0.04 |
| **ANOVA (p values)** | | | **0.001** | 0.027 | **0.001** | **0.001** | **0.001** | **0.001** | **0.001** | **0.001** | 0.002 | **0.001** | 0.742 |

MON—monsoon | POM—post-monsoon | PRM—pre-monsoon | WT—water temperature | DO—dissolved oxygen | Chl-a—chlorophyll-a | TSS—total suspended solids | $NO_3$—nitrate | $NO_2$—nitrite | $NH_3$—ammonia | IP—inorganic phosphate | Si—silicate | SD—standard deviation. ANOVA values given in bold represents significant difference ($p < 0.001$).

surfaces showed notable changes over time. Barnacles exhibited an initial peak in settlement (2.31 individuals/ $cm^2$) within the first 30 days on SS surfaces, but their numbers declined sharply subsequently, indicating early attachment followed by detachment, mortality, disturbance, overgrowth or competition with other fouling organisms. Settlement of polychaete tube worms, solitary ascidians, and green mussels gradually increased in density between 90 and 120 days. In terms of surface coverage, coelenterate hydroids dominated the initial phase (56.89%), covering nearly 80% of the surface from 0–60 days before declining. Following this, colonial ascidians peaked on the 90 day (24.44%), and declined after 120days (9.33%), replacing hydroids as the dominant organisms. Settlement of encrusting bryozoans was observed after 90 days (3.78%), and the recruits were observed on the coupons subsequently, but with a lower dominance compared to ascidians. Green mussels were observed to settle on the substrates from the $90^{th}$ day (0.11 individuals/$cm^2$) and peaked on the $120^{th}$ (1.12 individuals/$cm^2$) day. Settlement of green mussels was observed on empty barnacle shells and covered the entire coupon surface area on the outer layer, a trend which was observed in a previous study by Venkatnarayanan (2018). Species succession of foulants on SS surfaces was more prominent and dynamic compared to FRP surfaces.

Titanium surfaces exhibited a distinct biofouling pattern compared to (SS) and (FRP). On the SS surface, barnacles were the early settlers, within the first 30 days (1.40%). Subsequently, the surfaces were colonized by other fouling organisms such as polychaete worms, solitary ascidians, and green mussels showed a sporadic settlement with relatively lower fouling densities compared to SS and FRP. Results suggests that Ti resists dense fouling, likely due to its passive oxide layer, which makes it less appealing for biofouling attachment (Alshammari 2017). In terms of surface coverage, coelenterate hydroids, dominated during the initial 60 days (71.11%), and disappeared after 60 days.

Settlement of colonial ascidians also peaked around 90 (39.78%)–120 days (24.76%), similar to SS, but their presence was short-lived on Ti. Encrusting bryozoans were found in few numbers throughout the study period, further supporting the trend of lower fouling on Ti. Green mussels settled and dominated the fouling community after 120 days (0.92 individuals/$cm^2$) up to 300 days (0.72 individuals/$cm^2$). Similar to SS substrate, the presence of green mussels reduced the settlement of other organisms particularly barnacles, creating competitive pressure among species for space on the substrate. Overall, the relatively lower surface coverage on Ti indicates less biofouling accumulation compared to SS and FRP.

Fibre-reinforced plastic surfaces was found to accumulate higher biofouling compared to SS and Ti. Barnacle settlement peaked (1.77%), during the first 60 days of exposure. Additionally, green mussels and polychaete tube worms exhibit higher densities (0.92% and 0.40% respectively) on FRP, with continuous colonization observed after 120 days. Fibre-reinforced plastic supports a more diverse fouling community, likely due to its rougher surface texture and inert material composition, which provide more attachment points for organisms. In terms of surface coverage, coelenterate hydroids (20%), dominated along with barnacles during the early stages (first 60 days) but decline gradually, with the drop being less sharp than on SS and Ti. Colonial ascidians were found to appear later, peaking around 60 days (33.11%)–120 days (16.44%), and maintain a longer presence, suggesting that FRP provides a more stable environment for biofouling. Encrusting bryozoans were observed on the coupons and showed an increase in percentage coverage after 90 days (23.87%)–170 (10.67%) days, which was unique and not observed on SS and Ti surfaces. Green mussel density was notably high on this substrate, with spats beginning to attach from day 90 (0.34 individuals/$cm^2$) and steadily increasing, reaching a peak by 120 days (0.92 individuals/$cm^2$). In contrast, attachment on SS and Ti substrates was observed only after 120 days. Overall, the higher surface coverage on FRP suggests that it is the most prone to biofouling accumulation among the materials studied.

Hierarchical cluster analysis grouped the nine marine fouling species into four distinct clusters based on their standardized monthly abundance patterns shown in Figure 3. Although it does not display seasons explicitly, it reflects how closely species are aligned in terms of their temporal dynamics throughout the year. Species that are joined by short branches such as polychaete tube worms, oysters, and colonial ascidians exhibit similar seasonal trends, likely responding in comparable ways to environmental or ecological cues. In contrast, species like barnacles, solitary ascidians, and green mussels are separated by longer branch lengths, indicating distinctly different temporal behaviours. The stepwise clustering seen in the dendrogram highlights the presence of both tightly cohesive groups and more isolated taxa, providing insight into the degree of seasonal specialization or generalism.

Barnacles consistently appear as one of the most isolated species in the dendrograms, branching off at a large dissimilarity distance. This reflects their unique seasonal colonization pattern characterized by a distinct

**Table 3.** Pearson correlation between environmental parameters v/s biofouling load on each Substrate; Coloured grid - is the Pearson's value; (lowest value is mentioned in Green and the highest value is in Red, near to zero values are mentioned in tallow). Bold and black numbers with represent the p- value showing the significance at $p < 0.05$; normal numbers without bold do not have any significance. The stainless steel (SS), titanium (Ti), fibre-reinforced plastic (FRP) represents the fouling load during the three seasons.

| | WT | pH | Salinity | DO | Chl-a | TSS | $NO_2^-$ | $NO_3^-$ | $NH_4$ | IP | Si | SS | Ti | FRP |
|---|---|---|---|---|---|---|---|---|---|---|---|---|---|---|
| WT | | 0.101 | **0.001** | 0.023 | 0.146 | 0.286 | **0.012** | **0.022** | 0.075 | **0.022** | 0.993 | 0.678 | 0.363 | 0.776 |
| pH | -0.496 | | **0.008** | 0.001 | 0.184 | 0.142 | 0.209 | **0.019** | 0.164 | 0.079 | 0.293 | **0.002** | 0.159 | 0.048 |
| Salinity | 0.874 | -0.723 | | 0.001 | 0.145 | 0.077 | **0.007** | **0.003** | 0.013 | **0.013** | 0.840 | 0.156 | 0.900 | 0.565 |
| DO | -0.646 | 0.863 | -0.852 | | 0.173 | 0.136 | **0.026** | **0.001** | **0.020** | **0.018** | 0.684 | **0.034** | 0.557 | 0.206 |
| Chl-a | 0.446 | -0.411 | 0.447 | -0.421 | | 0.862 | 0.063 | 0.108 | 0.141 | **0.049** | 0.157 | 0.302 | 0.333 | 0.138 |
| TSS | -0.336 | 0.450 | -0.530 | 0.456 | -0.056 | | 0.079 | **0.027** | 0.068 | 0.295 | 0.512 | 0.234 | 0.751 | 0.621 |
| $NO_2^-$ | -0.696 | 0.391 | -0.730 | 0.636 | -0.551 | 0.527 | | **0.001** | **0.011** | **0.001** | 0.119 | 0.415 | 0.871 | 0.590 |
| $NO_3^-$ | -0.650 | 0.661 | -0.778 | 0.809 | -0.488 | 0.634 | 0.839 | | **0.001** | **0.011** | 0.322 | 0.215 | 0.983 | 0.505 |
| $NH_4$ | 0.532 | -0.429 | 0.691 | -0.659 | 0.451 | -0.543 | -0.704 | -0.843 | | 0.051 | 0.095 | 0.307 | 0.881 | 0.514 |
| IP | -0.649 | 0.526 | -0.692 | 0.667 | -0.578 | 0.330 | 0.844 | 0.700 | -0.575 | | 0.351 | 0.055 | 0.355 | 0.100 |
| Si | 0.003 | 0.331 | -0.065 | 0.131 | 0.436 | -0.210 | -0.475 | -0.313 | 0.504 | -0.295 | | 0.638 | 0.953 | 0.901 |
| SS | -0.134 | 0.789 | -0.436 | 0.613 | -0.326 | 0.372 | 0.260 | 0.386 | -0.322 | 0.566 | 0.152 | | **0.001** | **0.001** |
| Ti | 0.289 | 0.433 | 0.041 | 0.189 | -0.306 | 0.103 | -0.052 | 0.007 | -0.048 | 0.293 | -0.019 | 0.845 | | **0.001** |
| FRP | 0.092 | 0.580 | -0.185 | 0.393 | -0.455 | 0.159 | 0.173 | 0.214 | -0.209 | 0.497 | -0.040 | 0.918 | 0.961 | |

**Note:** Colour code presents the Pearson's values. WT—water temperature | DO—dissolved oxygen | Chl-a—chlorophyll-a | TSS—total suspended solids | $NO_3$—nitrate | $NO_2$—nitrite | $NH_3$—ammonia | IP—inorganic phosphate | Si—silicate

early-year peak (January–February) followed by a steep decline in their number through the rest of the year. Even though barnacles were year-round breeders at the tropical location, a peak in their settlement was observed in the months of January–February characterized by lower water temperatures. In all three dendrograms (Figure 3a,b,c), green mussels consistently appear as a distinct entity, clustering separately from other fouling species or joining groups only at high dissimilarity levels. This consistent isolation suggests that their seasonal abundance pattern is markedly different from the rest of the community. Unlike other taxa that exhibit synchronized settlement trends such as peaks during spring or declines in monsoon, green mussels show a unique temporal trajectory characterized by a decline in early spring followed by a steady increase through the summer and post-monsoon periods. This inverted pattern relative to species like solitary ascidians or barnacles likely reflects differences in ecological strategies, such as reproductive timing, settlement preferences, or environmental tolerance. As a result, their consistent unique status across all clustering analyses highlights their potential role as an indicator species for specific environmental conditions or seasonal shifts that are not captured by other taxa.

Solitary ascidians display a sharp spike in abundance during April and are otherwise low or negative throughout the year. Hydroids branch earlier in the clustering process and show a moderately distinct pattern, peaking early in the year (January–February) similar to barnacles and remaining low afterward. Polychaetes cluster more closely with species like oysters and ascidians, indicating moderately synchronized seasonal dynamics. Oysters follow a similar pattern to polychaete tube worms, showing moderate abundance through late spring and summer. Colonial ascidians exhibit mild abundance in PRM (March–May) and negligible presence afterward. Their limited seasonal window places them close to oysters and polychaetes in the dendrogram. Bryozoans show a brief spring peak (May), followed by low or absent values. They are structurally clustered with colonial ascidians, implying similar ecological timing.

The other species observed shows fluctuating presence without a sharp peak, resulting in a moderate position in the dendrogram. It clusters loosely with the mid-year species, reflecting variable and possibly opportunistic dynamics, possibly driven by less dominant or transient taxa. Based on the comparative analysis of the three dendrograms corresponding to SS, Ti, and FRP substrates, it is evident that FRP is the most favourable surface for the recruitment of green mussels. In the

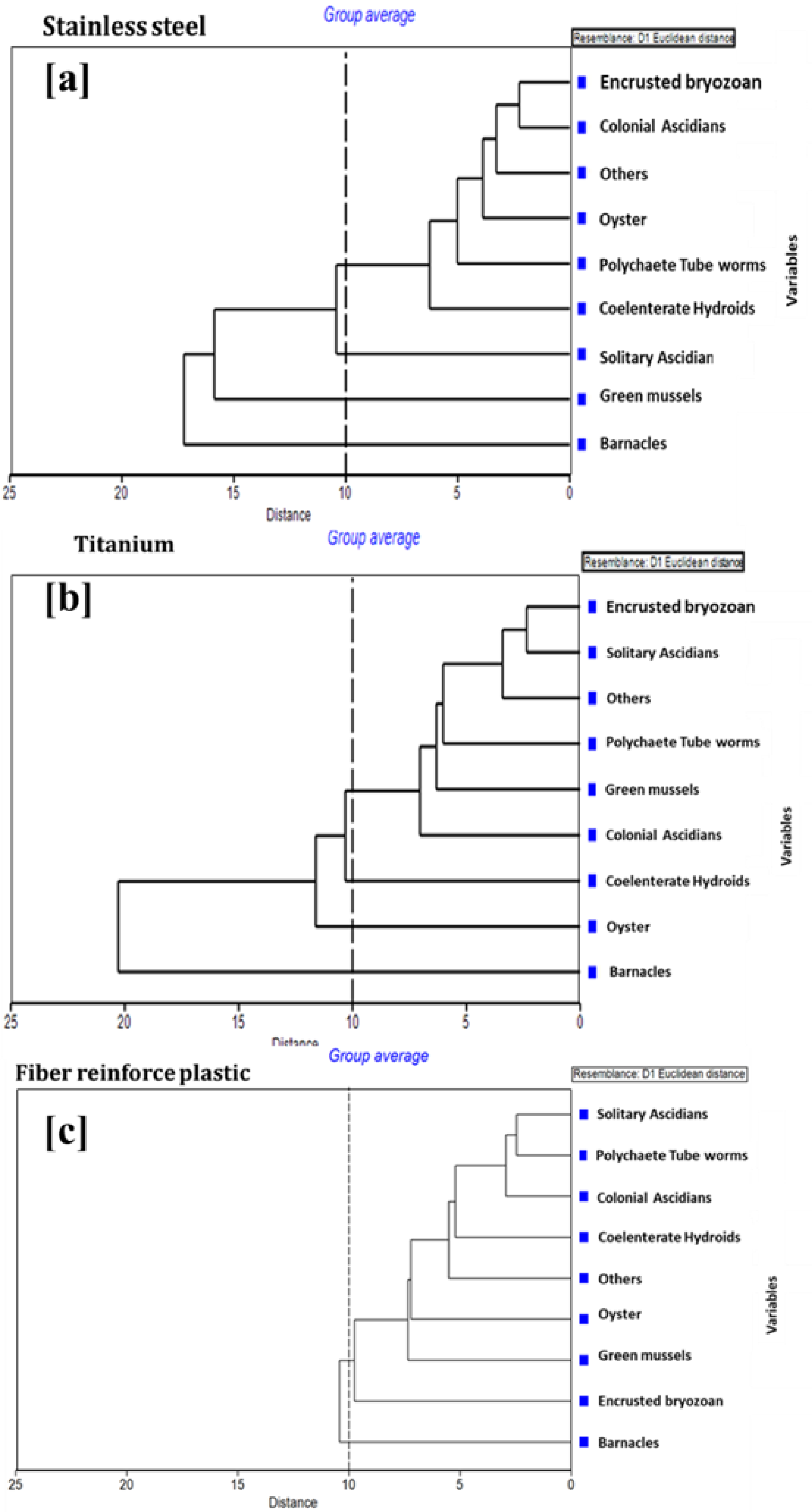


**Figure 3. Bray-Curtis similarities of species diversity in different materials (a) stainless steel, (b) titanium, & (c) fibre reinforced plastic in a year (Jan–Dec 2022).**

dendrogram for FRP, green mussels are less isolated and join clusters with other fouling species at a lower dissimilarity level. This suggests that their seasonal abundance pattern on FRP aligns more closely with the broader fouling community, indicating consistent and possibly robust recruitment.

In contrast, on SS, green mussels appear highly isolated in the dendrogram, branching off at a large dissimilarity distance. This implies that their occurrence on SS is ecologically distinct, likely reflecting limited settlement or poor substrate compatibility. Titanium shows an intermediate pattern, where green mussels still remain relatively isolated but to a lesser extent than on SS, suggesting moderate but less predictable recruitment. The overall trend points to FRP providing surface characteristics such as suitable roughness, favourable biofilm development, or lower material toxicity that better supports the settlement and establishment of green mussels compared to the other metallic substrates.

### Relationship between environmental parameters and fouling load in different coupons

#### Environmental parameters and correlations

Correlation matrix provides insight into the relationships between different water quality parameters and biofouling loading on coupons. Water temperature (WT) is strongly correlated with salinity (0.874, $p < 0.001$), Table 3. This could be due to the evaporation of water, which concentrates salts in the remaining water body. Conversely, dissolved oxygen (DO) and temperature exhibit a strong negative correlation (-0.646, $p = 0.023$), suggesting that higher temperatures reduce the solubility of oxygen in water. This is a well-documented phenomenon, as warmer water holds less oxygen, potentially leading to hypoxic conditions in aquatic ecosystems. Additionally, salinity and DO also show a significant negative correlation (-0.852, $p < 0.001$), indicating that areas with higher salinity tend to have lower oxygen levels, possibly due to reduced mixing or increased biological oxygen demand. pH was positively correlated with DO (0.863, $p < 0.001$). This could be due to increased photosynthetic activity in the water, which both raises pH (due to $CO_2$ uptake) and increases oxygen levels. On the other hand, pH and salinity have a negative correlation (-0.723, $p = 0.008$), suggesting that higher salinity waters tend to be more acidic. This could be due to the influence of dissolved salts and carbonate chemistry in marine or estuarine environments.

Among the inorganic nutrients a strong correlation between nitrite and nitrate (0.839, $p < 0.001$) was observed. Similarly, ammonium ($NH_4$) and nitrate have a strong inverse correlation (-0.843, $p < 0.001$), meaning that when ammonium concentrations are high, nitrate levels tend to be lower. This could indicate active nitrification, where ammonium is converted to nitrate through microbial processes. The overall pattern in these relationships points to active nitrogen cycling, likely influenced by biological activity and environmental conditions such as oxygen availability. Stainless steel is often used in marine environments due to its corrosion resistance, but does not inherently possess anti-fouling properties. Earlier studies with SS in seawater environments revealed that interaction of metals under neutral pH conditions results in an increase in electrostatic interactions, which can affect microbial adhesion, while alkaline conditions potentially accelerate surface oxidation (Ferris et al. 1989; Sedriks 1996).

Alternatively, it might indicate that SS structures are more commonly used in environments where pH is naturally higher. A decrease in pH reduces electrostatic interactions, thereby diminishing the free energy available for metallic ion adsorption (James & Healy 1972). Stainless steel corrosion is known to be affected by oxygen levels, as oxidation processes (such as the formation of chromium oxide protective layers) require oxygen (Kritzer 2004). Higher DO levels might enhance corrosion under certain conditions, especially in the presence of chlorides (Kritzer et al. 2000). Stainless steel can be prone to biofouling, but factors like surface roughness, passive oxide layer formation, and environmental conditions play a role.

#### Material-specific fouling and corrosion

Titanium is known for its excellent corrosion resistance in seawater due to its strong passive oxide layer ($TiO_2$), which reduces microbial attachment (Órdenes-Aenishanslins et al. 2014). Additionally, the photocatalytic properties of $TiO_2$ have been utilized for disinfection purpose, demonstrating antimicrobial activity under certain conditions (Simonin et al. 2016). Titanium is generally corrosion-resistant, but its interactions with dissolved organic matter, suspended solids, could initiate primary biofilm formation aiding settlement and colonization of higher organisms.

FRP surfaces are generally more prone to biofouling than metals due to their rough texture and ability to trap microorganisms. Several researchers have examined the adhesion of marine bacteria on various surfaces and concluded that bacterial attachment is lower on low-energy (hydrophilic) surfaces compare to high-energy surfaces, which promotes stronger adhesion (Dexter et al. 1975; Hamza et al. 1977). Muthukumar et al. (2011) reported that glass fibre reinforced polymer and carbon fibre reinforced showed maximum fouling (barnacle) attachment on hard surfaces (Muthukumar et al. 2011) than on flexible surfaces (Silicon rubber). FRP is the most prone to biofouling among the three due to its rough surface and micro plastic shedding, which can support microbial colonization.

**Green mussel settlement patterns**

Green mussel settlement was observed after 150 days and continues by covering the coupons completely. The attachment was seen during June–December with peak in August–September. In our study the first peak was lesser spat settlement. Green mussels dominating the whole surface area and not letting any other organisms to grow during this time. In previous report, it was observed that green mussel settlement during April–November with peaks in May–June, which showed some similarities to our current study carried out at the study area (Rajagopal et al. 1997; Sahu et al. 2011). It is also reported that the peak during March–November and with second peak August–September by (Paul 1942) Madras harbour. This peak settlement coincided with relative high temperature during the period (Selvaraj 1984). Myint & Tyler (1982) reported that spawning occurs according to the availability of food resources and high salinity. This indicates that more larval abundance and settlement pattern of green mussels influenced by the availability food, high temperature and salinity (Pieters et al. 1980; Newell et al. 1982).

**Implication of materials selection**

The present study highlights the significant differences in biofouling accumulation on SS, Ti, and FRP over time. Titanium is the most resistant material, while FRP shows the highest susceptibility to fouling, making it less favourable for long-term marine applications. Seasonal variations in fouling loads have also been reported in studies conducted at other locations (Swami & Chhapgar 2002; Swami & Udhayakumar 2010; Sahu et al. 2015). Understanding these material-specific trends is crucial for selecting appropriate materials for offshore structures, cooling water systems, and other marine applications where biofouling can impact performance and maintenance costs. When considering the other side of the story, it is important to recognize that the same materials that may be prone to biofouling can also serve as valuable substrates for recruiting desired marine organisms for aquaculture purposes. Among the three substrates used for recruitment studies, Ti remained to be highly resistant to fouling. However, stainless steel, with its moderate resistance to fouling, may offer a balanced substrate for attracting certain species, particularly those that thrive in semi-clean environments. Its ability to support a variety of organisms, from barnacles to algae, can be advantageous for applications like marine habitats or artificial reefs where biodiversity is desired.

## CONCLUSION

In conclusion, the comparative analysis of the materials reveals distinct differences in their susceptibility to biofouling as well as species succession patterns. Among the three surfaces, evaluated titanium showed the least biofouling with a low density of fouling organisms and minimal surface coverage, highlighting its resistance to biofouling. Stainless steel surfaces on the other hand, experienced moderate fouling, with barnacles settling early but eventually their numbers decreased as settlement of other organisms occurred, leading to a more balanced fouling community over time. In contrast, FRP was found to be a most suitable substrate for settlement and recruitment of many biofouling organisms and was found to support a higher density of organisms due to its inert nature and rough surface. Ideally barnacles were the initial settlers on all three surfaces during the first 30 days of exposure followed by coelenterate hydroids which dominated the surfaces after 30 days of immersion. Colonial and mat forming ascidians, solitary bryozoans settled and colonized from the 60$^{th}$ day. Green mussels formed the mature fouling community with on all three surfaces with settlement observed from 120 day. Results of the study provide the biofouling potential of these three surfaces and FRP surfaces was found to sustain a more diverse fouling community.

## REFERENCES

**Achary, M.S., G. Sahu, A.K. Mohanty, M.K. Samatara, S.N. Panigrahy, M. Selvanayagam, K.K. Satpathy, M.V.R. Prasad & R.C. Panigrahy (2010)**. Phytoplankton abundance and diversity in the coastal waters of Kalpakkam, east coast of India in relation to the environmental variables. *The Bioscan* 2: 553–568.

**Alshammari, Y.N. (2017)**. Production and characterization of titanium-based alloys with potential for antifouling and biofouling. Doctoral dissertation, University of Waikato.

**APHA (2005)**. Standard Methods for the Examination of Water and Wastewater, 21$^{st}$ edition. American Public Health Association. American Works Association and Water Environmental Federation, Washington, D.C.

**Alayande, A.B., J. Lim, J. Kim, S. Hong, A.S. Al-Amoudi & B. Park**

(2022). Fouling control in SWRO desalination during harmful algal blooms: A historical review and future developments. *Desalination* 543: 116094. https://doi.org/10.1016/j.desal.2022.116094

**Alotaibi, G.F., & M.A. Bukhari (2021)**. Factors influencing bacterial biofilm formation and development. *American Journal of Biomedical Science & Res*earch 12(6): 617–626. https://doi.org/10.34297/AJBSR.2021.12.001820

**Azis, P.A., I. Al-Tisan & N. Sasikumar (2001)**. Biofouling potential and environmental factors of seawater at a desalination plant intake. *Desalination* 135(1–3): 69–82.

**Briand, J.F., A. Barani, C. Garnier, K. Réhel, F. Urvois, C. Le Poupon & C. Bressy (2017)**. Spatio-temporal variations of marine biofilm communities colonizing artificial substrata including antifouling coatings in contrasted French coastal environments. *Microbial Ecology* 74: 585–598.

**Briand, J.F., T. Pollet, B. Misson, C. Garnier, M. Lejars, M. Maintenay & C. Bressy (2022)**. Surface characteristics together with environmental conditions shape marine biofilm dynamics in coastal NW Mediterranean locations. *Frontiers in Marine Science* 8: 746383. https://doi.org/10.3389/fmars.2021.746383

**Callow, M.E. & J.A. Callow (2011)**. Trends in the development of environmentally friendly fouling-resistant marine coatings. *Nature Communications* 2: 244. https://doi.org/10.1038/ncomms1251

**Decho, A.W. & T. Gutierrez (2017)**. Microbial extracellular polymeric substances (EPSs) in ocean systems. *Frontiers in microbiology* 8: 922. https://doi.org/10.3389/fmicb.2017.00922

**Dexter, S.C., J.D. Sullivan, J. Williams & S.W. Watson (1975)**. Influence of substrate wettability on the attachment of marine bacteria to various surfaces. *Applied and Environmental Microbiology* 30: 298–308.

**Dexter, S.C. & P. Chandrasekaran (1998)**. Corrosion and biofouling of metals in marine environments. *Biofouling* 12: 3–20.

**Dobretsov, S. (2010)**. *Marine Biofouling: Colonization Processes and Defenses*. Springer-Verlag, 316 pp.

**Dobretsov, S., J.C. Thomason & P.Y. Qian (2013)**. *Biofouling: Processes, Ecological Consequences and Control.* Springer, Berlin, Heidelberg. https://doi.org/10.1007/978-3-642-76543-8_2

**Deser, C., M.A. Alexander, S.P. Xie & A.S. Phillips (2010)**. Sea surface temperature variability: Patterns and mechanisms. *Annual Review of Marine Science* 2(1): 115–143.

**Dürr, S. & D.I. Watson (2010)**. Biofouling and antifouling in aquaculture. *Biofouling* 12: 267–287.

**Fernandes, J.A., L. Santos, T. Vance, T. Fileman, D. Smith, J.D. Bishop & M.C. Austen (2016).** Costs and benefits to European shipping of ballast-water and hull-fouling treatment: Impacts of native and non-indigenous species. *Marine Policy* 64: 148–155. https://doi.org/10.1016/j.marpol.2015.11.015

**Fernández-González, C., G.A. Tarran, N. Schuback, E.M.S. Woodward, J. Arístegui & E. Marañón (2022).** Phytoplankton responses to changing temperature and nutrient availability are consistent across the tropical and subtropical Atlantic. *Communications Biology* 5(1): 1035. https://doi.org/10.1038/s42003-022-03971-z

**Ferris, F. G., S. Schultze, T.C. Witten, W.S. Fyfe & T.J. Beveridge (1989)**. Metal interactions with microbial biofilms in acidic and neutral pH environments. *Applied and Environmental Microbiology* 55(5): 1249–1257.

**Fitridge, I., T. Dempster, J. Guenther, R. de Nys (2012)**. The impact and control of biofouling in marine aquaculture: a review. *Biofouling* 28: 649–669.

**Grasshoff, K., K. Kremling, M. Ehrhardt (Eds.). (1999)**. *Methods of Seawater Analysis. 3rd Edition*. Wiley-VCH, Weinheim, 632 pp.

**Hadfield, M.G. (2011**). Biofilms and marine invertebrate larvae: what bacteria produce that larvae use to choose settlement sites. *Annual Reviews on Marine Science* 3: 453–470. https://doi.org/10.1146/annurev-marine-120709-142753

**Hammer, Ø., D.A.T. Harper & P.D. Ryan (2001).** PAST: Paleontological Statistics Software Package for Education and Data Analysis. *Palaeontologia Electronica* 4(1): 9.

**Hamza, A., V.A. Pham, T. Matsuura, & J.P. Santerre (1997)**. Development of membranes with low surface energy to reduce the fouling in ultrafiltration applications. *Journal of Membrane Science* 131(1–2): 217–227.

**Henderson, P. (2010)**. Fouling and antifouling in other industries – power stations, desalination plants – drinking water supplies and sensors, pp. 288–305. In: Durr, S. & J.C. Thomason (eds.). *Biofouling.* Wiley-Blackwell, Singapore, 464 pp.

**Hopkins, G., I. Davidson, E. Georgiades, O. Floerl, D. Morrisey & P. Cahill (2021).** Managing biofouling on submerged static artificial structures in the marine environment–assessment of current and emerging approaches. *Frontiers in Marine Science* 8: 759194. https://doi.org/10.3389/fmars.2021.759194

**James, R.O. & T.W. Healy (1972)**. Adsorption of hydrolysable metal ions at the oxide—water interface. III. A thermodynamic model of adsorption. *Journal of Colloid and Interface Science* 40(1): 65–81.

**Jamieson, T. & S.C. Leterme (2021)**. Influences and impacts of biofouling in SWRO desalination plants. *Critical Reviews in Environmental Science and Technology* 51(12): 1281–1301.

**Kobayashi, M. & R.H. Dauskardt (2001)**. Corrosion and biofouling resistance of titanium alloys in marine environments. *Journal of Materials Science* 36: 5681–5688.

**Kritzer, P., N. Boukis & E. Dinjus (2000)**. Review of the corrosion of nickel-based alloys and stainless steels in strongly oxidizing pressurized high-temperature solutions at subcritical and supercritical temperatures. *Corrosion* 56(11): 1093–1104.

**Kritzer, P. (2004).** Corrosion in high-temperature and supercritical water and aqueous solutions: a review. *The Journal of Supercritical Fluids* 29(1–2): 1–29.

**Maki, J.S. & R. Mitchell (2002)**. Biofouling in the marine environment, pp. 610–619. In: Bitton G. (eds.). *Encyclopaedia of Environmental Microbiology.* Wiley, New York, 3730 pp.

**More, T.T., J.S.S. Yadav, S. Yan, R.D. Tyagi & R.Y. Surampalli (2014)**. Extracellular polymeric substances of bacteria and their potential environmental applications. *Journal of Environmental Management* 144: 1–25. https://doi.org/10.1016/j.jenvman.2014.05.010

**Murthy, P.S., P. Veeramani, M.I.M. Ershath & V.P. Venugopalan (2011).** Biofouling evaluation in the seawater cooling circuit of an operating coastal power plant. *Power Plant Chemistry* 13(6): 314–319.

**Muthukumar, T., A. Aravinthan, K. Lakshmi, R. Venkatesan, L. Vedaprakash & M. Doble (2011)**. Fouling and stability of polymers and composites in marine environment. International *Biodeterioration & Biodegradation* 65(2): 276–284. https://doi.org/10.1016/j.ibiod.2010.11.012

**Myint, U.M. & P.A. Tyler (1982)**. Effects of temperature, nutritive and metal stressors on the reproductive biology of Mytilus edulis. *Marine Biology* 67: 209–223.

**Nair, K.V.K., P. Murugan & M.S. Eswaran (1998).** Macrofoulants in Kalpakkam coastal waters, east coast of India, *Indian Journal of Marine Sciences* 17: 341–343.

**Nair, K.V.K. (1999)**. Marine biofouling and its control with particular reference to condenser-cooling circuits of power plants-an overview. *Journal of the Indian Institute of Science* 79(6): 497.

**Negm, N.A., D.A. Ismail, S.A. Moustafa & M.T.A. Kana (2019)**. Adhesion of Bacteria to Solid Surfaces. *Surfactants in Tribology* 6: 131–159.

**Newell, R.I., T.J. Hilbish, R.K. Koehn & C.J. Newell (1982)**. Temporal variation in the reproductive cycle of Mytilus edulis L. (Bivalvia, Mytilidae) from localities on the east coast of the United States. *The Biological Bulletin* 162(3): 299–310.

**Órdenes-Aenishanslins, N.A., L.A. Saona, V.M. Durán-Toro, J.P. Monrás, D.M. Bravo & J.M. Pérez-Donoso (2014)**. Use of titanium dioxide nanoparticles biosynthesized by Bacillus mycoides in quantum dot sensitized solar cells. *Microbial Cell Factories* 13: 1–10.

**Page, H.M., J.E. Dugan & F. Pilts (2010)**. Fouling and antifouling in oil and other offshore industries, pp. 252–266. In: Durr, S. & J.C. Thomason (eds.). *Biofouling.* Wiley-Blackwell, Singapore, 464 pp.

**Patil, J.S., A.C. Anil & R. Harke (2007).** Biofouling community structure on different substrates in a tropical estuary. *Biofouling* 23(6): 415–427.

**Paul, M.D. (1942).** Studies on the growth and breeding of certain sedentary organisms in the Madras harbour. *Indian Academy of Sciences-Section B* 15: 1–42.

**Pieters, H., J.H. Kluytmans, D.I. Zandee & G.C. Cadee (1980)**. Tissue composition and reproduction of Mytilus edulis in relation to food availability. *Netherlands Journal of Sea Research* 14(3–4): 349–361.

**Ponnusamy, V., S. Venkatnarayanan & R. Nandakumar (2016)**. Seasonal variation of biofouling communities along the southeast coast of India. *Indian Journal of Geo-Marine Sciences* 45(5): 652–660.

**Ponnusamy, K., S. Munilkumar, S. Das, A. Verma, R. Venkitesan & A.K. Pal (2017)**. Shellfish resources around Madras Atomic Power Station Kalpakkam, Southeast India. *Journal of Asia-Pacific Biodiversity* 10(1): 118–123.

**Qian, P.Y., S.C.K. Lau, H.U. Dahms, S. Dobretsov & T. Harder (2007)**. Marine biofilm as mediator of colonization by marine macroorganisms: implications for antifouling and aquaculture. *Marine Biotechnology* 9: 399–410.

**Qian, P. Y., A. Cheng, R. Wang & R. Zhang (2022)**. Marine biofilms: diversity, interactions and biofouling. *Nature Reviews Microbiology* 20(11): 671–684. https://doi.org/10.1038/s41579-022-00744-7

**Rajagopal, S., N. Sasikumar J. Azariah, K.V.K. Nair (1991)**. Some observations on biofouling in the cooling water conduits of a coastal power plant. *Biofouling* 3: 311–324.

**Rajagopal, S., K.V.K. Nair, G. Van der Velde & H.A. Jenner (1997)**. Seasonal settlement and succession of fouling communities in Kalpakkam, east coast of India. *Netherland Journal of Aquatic Ecology* 30: 309–325.

**Rao, T.S. (2015)**. Biofouling in industrial water systems, pp. 123–140. In: Amjad, Z. & K.D. Demadis (eds.). *Mineral Scales and Deposits*. Elsevier, 739 pp.

**Rao, S.T., P.S. Murthy, P. Veeramani, D.S. Narayanan, R. Ramesh, B.N. Jyothi & G.A. Ramadass (2021).** Assessment of bio growth assemblages with depth in a seawater intake system of a coastal power station. *Biofouling* 37(5): 506–520.

**Sahu, G., M.S. Achary, K.K. Satpathy, A.K. Mohanty, S. Biswas & M.V.R. Prasad (2011)**. Studies on the settlement and succession of macrofouling organisms in the Kalpakkam coastal waters, southeast coast of India. *Indian Journal of Geo-Marine Sciences* 40(6): 747.

**Sahu, G., K.K. Satpathy, A.K. Mohanty & S.K. Sarkar (2012)**. Variations in community structure of phytoplankton in relation to physicochemical properties of coastal waters, southeast coast of India. *Indian Journal of Geo-Marine Sciences* 41(3): 223–241.

**Sahu, G., K.K. Satpathy, A.K. Mohanty, S. Biswas, M.S. Achary & S. Sarkar (2013)**. Larval abundance and its relation to macrofouling settlement pattern in the coastal waters of Kalpakkam, southeastern part of India. *Environmental Monitoring and Assessment* 185: 1951–1967.

**Sahu, G., A.K. Mohanty, M.S. Achary, M.V.R. Prasad & K.K. Satpathy (2015)**. Recruitment of biofouling community in coastal waters of Kalpakkam, south-western Bay of Bengal, India. *Indian Journal of Geo-Marine Sciences* 44(9): 1335–1351.

**Satpathy, K.K. (1996).** Seasonal distribution of nutrients in the coastal waters of Kalpakkam, East Coast of India. *Indian Journal of Geo-Marine Science* 25: 221–224.

**Satpathy, K.K., A.K. Mohanty, G. Sahu, S. Biswas, M.V.R. Prasad & M. Slvanayagam (2010).** Biofouling and its control in seawater cooled power plant cooling water system-a review, pp. 191–242. In: Tsvetkov, P. (ed.). *Nuclear Power*. IntechOpen. 398 pp.

**Satheesh, S. & S.G. Wesley (2009)**. Impact of December 26, 2004 tsunami on the hydrobiology of Kudankulam coast, Gulf of Mannar, India. *Environmental Monitoring and Assessment* 156: 131–139.

**Sanders, P.F. & P.J. Sturman (2005)**. Biofouling in the oil industry. *Petroleum Microbiology* 1: 171–198. https://doi.org/10.1128/9781555817589.ch9

**Schultz, M.P., J.A. Bendick, E.R. Holm & W.M. Hertel (2011)**. Economic impact of biofouling on a naval surface ship. *Biofouling* 27: 87–98.

**Sedriks, A.J. (1996)**. *Corrosion of Stainless Steels*. John Wiley & Sons.

**Selvaraj, V. (1984)**. Community Structure in the Coastal Ecosystem with Special Reference to the Green Mussel *Perna Viridis* (Linnaeus). Doctoral dissertation, University of Madras, Madras.

**Shevalkar, M., A. Mishra & S.S. Meenambiga (2020)**. A review on invasive species in marine biofouling. *Research Journal of Pharmacy and Technology* 13(9): 4517–4521.

**Simonin, M., A. Richaume, J.P. Guyonnet, A. Dubost, J.M. Martins & T. Pommier (2016)**. Titanium dioxide nanoparticles strongly impact soil microbial function by affecting archaeal nitrifiers. *Scientific Reports* 6(1): 33643. https://doi.org/10.1038/srep33643

**Suryanarayan, A. & D.P. Rao (1992)**. Coastal circulation and upwelling index along the east coast of India, pp. 125–129. In: *Physical Process in Indian Seas.* Proceedings of first Convention (ISPSO).

**Swami, B.S. & B.F. Chhapgar (2002).** Settlement pattern of Ascidians in harbour waters of Mumbai, west coast of India. *Indian Journal of Marine Science* 31: 207–212.

**Swami, B.S. & M. Udhayakumar (2010).** Seasonal influence on settlement, distribution and diversity of fouling organisms at Mumbai harbour. *Indian Journal of Marine Science* 39: 57–67.

**Todd, P.A., E.C. Heery, L.H. Loke, R.H. Thurstan, D.J. Kotze & C. Swan (2019)**. Towards an urban marine ecology: characterizing the drivers, patterns and processes of marine ecosystems in coastal cities. *Oikos* 128(9): 1215–1242.

**Varkey, M.J., V.S.N. Murty & A. Suryanarayana (1996).** Physical oceanography of the Bay of Bengal and Andaman Sea. *Oceanography and Marine Biology: An Annual Review* 34: 1–70.

**Venkataraman, K., C. Raghunathan, R. Raghuraman & C.R. Sreeraj (2012)**. *Marine Biodiversity in India*. Zoological Survey of India, Kolkata, 168 pp.

**Venkatnarayanan, S. (2018**). Studies on Inhibition of Amphibalanus reticulatus (Utinomi) Larval Settlement and Development of Novel Antifouling Approaches. PhD thesis submitted to University of Madras, Chennai, Tamil Nadu, India.

**Venugopalan, V.P., S. Rajagopal, N. Sasikumar & K.V.K. Nair (1991)**. Marine biology of a seawater tunnel on the east coast of India, pp. 253–259. In: *Oceanography of the Indian Ocean*. Oxford & IBH Publishers, New Delhi, 788 pp.

**Venkatesan, R., P. Senthilkumar, N. Vedachalam & P. Murugesh (2017)**. Biofouling and its effects in sensor mounted moored observatory system in Northern Indian Ocean. *International Biodeterioration & Biodegradation* 116: 198–204. https://doi.org/10.1016/j.ibiod.2016.10.034

**Wahl, M. (2020)**. Living attached: aufwuchs, fouling, epibiosis, pp. 31–83. In: Nagabhushanam, R. (ed.). *Fouling Organisms of the Indian Ocean*. CRC Press, 550 pp.

**Wickramasinghe, M.P., K.A.M. Sudarshani & H.C.E. Wegiriya (2021)**. The diversity of marine invertebrate macrofauna in selected rocky intertidal zones of Matara, Sri Lanka. *Asian Journal of Conservation Biology* 10(1): 15–21.

**Wigglesworth-Cooksey, B. & K.E. Cooksey (2005)**. Use of fluorophore-conjugated lectins to study cell-cell interactions in model marine biofilms. *Applied Environmental Microbiology* 71(1): 428–435. https://doi.org/10.1128/aem.71.1.428-435.2005

**Yeo, D.C., S.T. Ahyong, D.M. Lodge, P.K. Ng, T. Naruse & D.J. Lane (2009)**. Semisubmersible oil platforms: understudied and potentially major vectors of biofouling-mediated invasions. *Biofouling* 26(2): 179–186.

**Yousef, A. & A. Nasser (2023)**. Examining the Effects of Bio Fouling on Ships and How It Contributes to the Introduction of Non-native Species in Newly Discovered Coastal Areas in Bio Fouling on Ship Hulls and Its Ecological Ramification. *SSRN Electronic Journal* January: 1–24. https://doi.org/10.2139/ssrn.4666557

**Zhao, Q., Y. Liu & C. Wang (2014)**. Effect of surface roughness and hydrophobicity on marine bacterial adhesion. *Colloids and Surfaces B: Biointerfaces* 113: 1–8.

**Zhang, H., W. Cao, Z. Wu, X. Song, J. Wang & T. Yan (2015)**. Biofouling on deep-sea submersible buoy systems off Xisha and Dongsha islands in the northern South China Sea. *International Journal of Biodeterioration and Biodegradation* 104: 92–96. https://doi.org/10.1016/j.ibiod.2015.05.003

The opinions expressed by the authors do not reflect the views of the Journal of Threatened Taxa, Wildlife Information Liaison Development Society, Zoo Outreach Organization, or any of the partners. The journal, the publisher, the host, and the partners are not responsible for the accuracy of the political boundaries shown in the maps by the authors.

**Journal of Threatened Taxa** is indexed/abstracted in Bibliography of Systematic Mycology, Biological Abstracts, BIOSIS Previews, CAB Abstracts, EBSCO, Google Scholar, Index Copernicus, Index Fungorum, JournalSeek, National Academy of Agricultural Sciences, NewJour, OCLC WorldCat, SCOPUS, Stanford University Libraries, Virtual Library of Biology, Zoological Records.

NAAS rating (India) 5.64

Print copies of the Journal are available at cost. Write to:
The Managing Editor, JoTT,
c/o Wildlife Information Liaison Development Society,
3A2 Varadarajulu Nagar, FCI Road, Ganapathy, Coimbatore,
Tamil Nadu 641006, India
ravi@threatenedtaxa.org & ravi@zooreach.org

www.threatenedtaxa.org

OPEN ACCESS



**ISSN 0974-7907 (Online) | ISSN 0974-7893 (Print)**

**May 2026 | Vol. 18 | No. 5 | Pages: 28739–29002**
**Date of Publication: 26 May 2026 (Online & Print)**
**DOI: 10.11609/jott.2026.18.5.28739-29002**

### Articles



### Communications



### Review



### Short Communications



### Notes



**Publisher & Host**

Threatened Taxa